

# Mathematical sciences

## The dynamics of Colliding Galaxies

P.M.S.Namboodiri  
Indian Institute of Astrophysics  
Bangalore 560034 India  
E-mail:pmsn@iiap.res.in

### Abstract

Galaxies interact in a multitude of ways with their environment. Such interactions can alter the morphological type of galaxies, trigger star formation and even produce active galactic nuclei. During the past three decades computer simulations have been extensively used to study the dynamics of colliding galaxies. Galactic collision is essentially an N-body problem where N represents the number stars in a galaxy. The most important parameter in a galaxy collision is the impact parameter. Numerical simulations have been performed to study the effect of changing the impact parameter in a galactic collision. The density distribution in the galaxy corresponds to that of a polytrope of index  $n = 4$ . Both merging and non-merging collisions of galaxies have been studied to see where the transition occurs between these two processes. Merging occurs when the distance of closest approach of the galaxies is less than three times its half-mass radius. The density profiles of the merger remnants follow a  $r^{1/4}$  law. Distant encounters do not result in merging and the galaxies remain almost in tact with only negligible change in its mass and internal energy.

**Key words:** galaxies, dynamics, collisions, numerical simulations

### 1.Introduction

Galaxies are known to interact in a multitude of ways with their environment. The environment plays an important role in shaping the structure of a galaxy. Galaxies with close companions are expected to merge in a few crossing times. Collisions of galaxies of comparable mass that are widely separated do not coalesce in a Hubble time. Giant luminous galaxies at the cores of dense clusters are supposed to have formed by the merger of smaller companions.

Merging and disruption are two important processes in the dynamical evolution of a binary stellar system. The ratio of the times of disruption and merging is given by

$$\frac{t_d}{t_m} \approx \frac{6}{(n-5)} \frac{a}{R} \frac{M}{M_1} \quad (1)$$

---

Invited talk at Indian Science Congress Hyderabad, 3 – 7 January 2006

where  $t_d$  and  $t_m$  are the disruption and merging times  $a$  is the orbital radius,  $R$  is the radius of the galaxy with mass  $M$ ,  $M_1$  is the mass of the perturber and  $n$  is the polytropic index describing the density distribution of the galaxy [1]. It may be noted that if the galaxies are centrally concentrated (i.e.,  $n = 4$ ) and have similar masses, merger occurs more rapidly than disruption. On the other hand, if the masses are dissimilar, the interaction between them is likely to cause considerable disruption to the less massive companion and in this case the disruption time could be shorter than the merging time.

Elliptical galaxies constitute about 10 per cent of any remarkable complete survey of binary galaxies. They are almost gas free systems so that the effects of gas dynamics can be neglected. Bound elliptical pairs tend to have similar mass and their separation and velocity difference are small compared to other types of galaxy pairs [2]. Hence they are well posed for numerical simulations. Most of the earlier simulations considered merging collisions of equal mass spherical galaxies [3 – 22]. The present work considers collisions of equal mass galaxies where the density distribution of the galaxies is represented by that of a polytrope with index  $n = 4$ . This is considered to be appropriate for the typical density distribution of a real elliptical galaxy. Both merging and non-merging simulations have been performed to obtain an idea about the transition region between the two phenomenon. The numerical model of the present work is described in Section 2. The results are presented and discussed in Section 3 and the conclusions are given in Section 4.

## 2. Initial conditions

A pair of equal mass galaxies with mass  $M$  is considered. The density distribution of  $M$  correspond to that of  $n = 4$  polytrope which is typical of the density distribution of an elliptical galaxy. The galaxy consists of a number of particles  $N$  where  $N = 5000$ . The motion of the individual particles is governed by the equation

$$\ddot{\mathbf{r}}_i = -G \sum_{\substack{j=1 \\ j \neq i}}^N \frac{m_j}{r_{ij}^3} \mathbf{r}_{ij}, \quad i = 1, 2, 3, \dots, N \quad (2)$$

where  $\mathbf{r}_i$  is the position vector of the  $i^{\text{th}}$  particle in an inertial frame of reference,  $m_i$  its mass and  $G$  is the gravitational constant. The calculation of the force on one particle requires the knowledge of the position of all the other particles in the system as a result of which the computing time goes as  $N^2$ . This time becomes prohibitively expensive even for a modest value of  $N$  and hence restricts the study of systems with large  $N$ . Further the force becomes very large if two particles come close together. To avoid this difficulty we use a softened potential for each particle given by

$$\Phi_i = -G \sum \frac{m_j}{(r_{ij}^2 + \varepsilon^2)^{1/2}} \quad (3)$$

The quantity  $\varepsilon$  is called the softening parameter and it is taken to be less than  $RN^{-1/3}$  where  $R$  is the radius of the galaxy. We have chosen a system of units in which  $G = M = 1$ . If we take  $M = 10^{11} M_\odot$  and  $L = 10$  kpc, the unit of time is  $4.7 \times 10^6$  yr and the unit of

velocity is approximately 208 km/sec. Accordingly the softening parameter turns out to be 100 pc. The initial model has a radius of 45 kpc and its half-mass radius  $R_h$  is 8.3 kpc. 10 per cent of the mass is within 3 kpc and 90 per cent of the mass, within  $2 R_h$  and so the galaxy is a centrally concentrated one. The crossing time  $t_{cr} = 2R_h / \langle \bar{v}^2 \rangle^{1/2}$  where  $\langle \bar{v}^2 \rangle^{1/2}$  is the internal mean velocity and it is about 2.8 units. The galaxy is close to virial equilibrium and possesses no net angular momentum. The important parameters in a galaxy – galaxy collision are the impact parameter, the relative velocity of the orbit and the mass ratio of the galaxies. The dynamically significant parameter corresponding to the impact parameter is the distance of closest approach  $p$  of the orbit. The merging of the galaxy occurs rarely for high velocity distant encounters. On the other hand galaxies that are bound to each other are expected to merge in a few orbital periods. The interaction is expected to strong when the galaxies undergo collision on a marginally bound or parabolic orbit. Consequently we have taken the initial relative orbit of the galaxies to be parabolic.

Two similar galaxies are placed with an initial separation large enough so that at this distance the tidal forces are negligible compared to the internal gravitational force in a system We use different values for the impact parameter such that  $p/R_h = 0.5, 1, 2.5, 3, 4, 5, 6, 7.5, \text{ and } 10$  and these models are respectively denoted by P1, P2, ..., P9. The two galaxies are moving in relative parabolic orbit with x-y plane coinciding with the orbital plane. The computations are performed till the galaxies merged in close collisions or till the galaxies become detached and showed tendency to recede from each other. The equations of motion are integrated using the special purpose GRAPE computer system [23]. The collision parameters are given in table 1.

Table 1. Collision parameters and results

Model	$p/R_h$	$V_p/V_e$	$\Delta U/ U $	$\Delta M/M$	$(\Delta M/M)_e$
P1	0.5	0.482	1.033	0.173	0.186
P2	1.0	0.575	1.011	0.166	0.193
P3	2.5	1.023	1.016	0.161	0.218
P4	3.0	1.102	1.030	0.182	0.220
P5	4.0	1.214	0.457	0.077	-
P6	5.0	1.435	0.435	0.043	-
P7	6.0	1.518	0.436	0.055	-
P8	7.5	1.731	0.427	0.047	-
P9	10.0	2.032	0.431	0.048	-

### 3. Results and discussion

#### 3.1 General feature

In our models P1 – P4 represent closely colliding galaxies where as P5 – P9 are distant collisions. In close collisions there is significant loss in the orbital energy of the galaxies as a result of which the orbit shrinks and the two galaxies ultimately merge. In distant

collisions loss in orbital energy is negligible and the galaxies recede from each other after their closest approach time. The general features of the galaxies during the collisions are shown in fig. 1. This figure shows the projections of the particles in the orbital plane i.e., the x-y plane, for selected times. In this figure the horizontal panels from top to bottom represent models P1, P2, P6 and P7 respectively. The second figure in each model shows the galaxies very near to their close collision. It may be noted that the first two models merge by  $t = 15t_{cr}$  and remain as a single system till the end of computation where as in the last two models, the galaxies become completely detached by  $t = 50t_{cr}$  and their separations increases afterwards. Similar behaviour is observed in other non-merging models also.

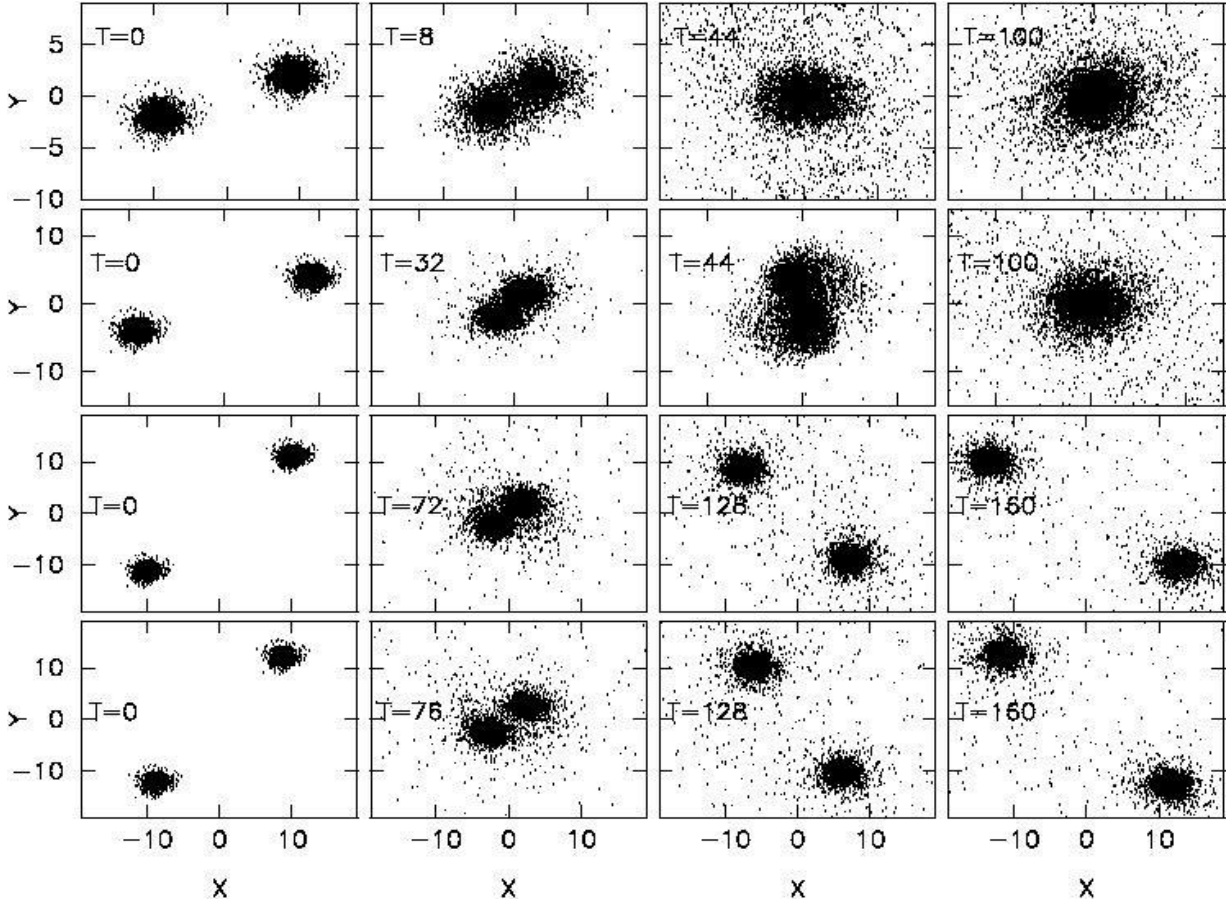


Figure 1. Projections of particles in the orbital plane at selected times. The rows from top to bottom represent models P1, P2, P6 and P7.

### 3.2 Merging criterion

Models P1 – P4 merge in less than 15 crossing time and models P5 – P9 do not merge even after 60 crossing times. Earlier numerical simulations have shown that in a head-on collision, merging occurs when the collision velocity at minimum separation  $V_p < 1.16V_e$  where  $V_e$  is the escape velocity at that distance [24]. This is in agreement with our results as can be seen from table 1 where we have tabulated the values of  $V_p/V_e$ . Clearly for

merging simulations the values of  $V_p/V_e < 1.2$ . [4] has shown that merging of spherical galaxies occur when the galaxies overlap significantly at closest approach such  $p < 2.5R_h$ . It can be seen from table 1 that for centrally concentrated galaxies merging takes place when  $p < 3R_h$  which is satisfied by models P1 – P4. This implies that a knowledge of the values of  $p/R_h$  together with  $V_p/V_e$  in principle will determine the fate of a galactic collision. The merging process depends strongly first on the impact parameter and then on the velocity of collision.

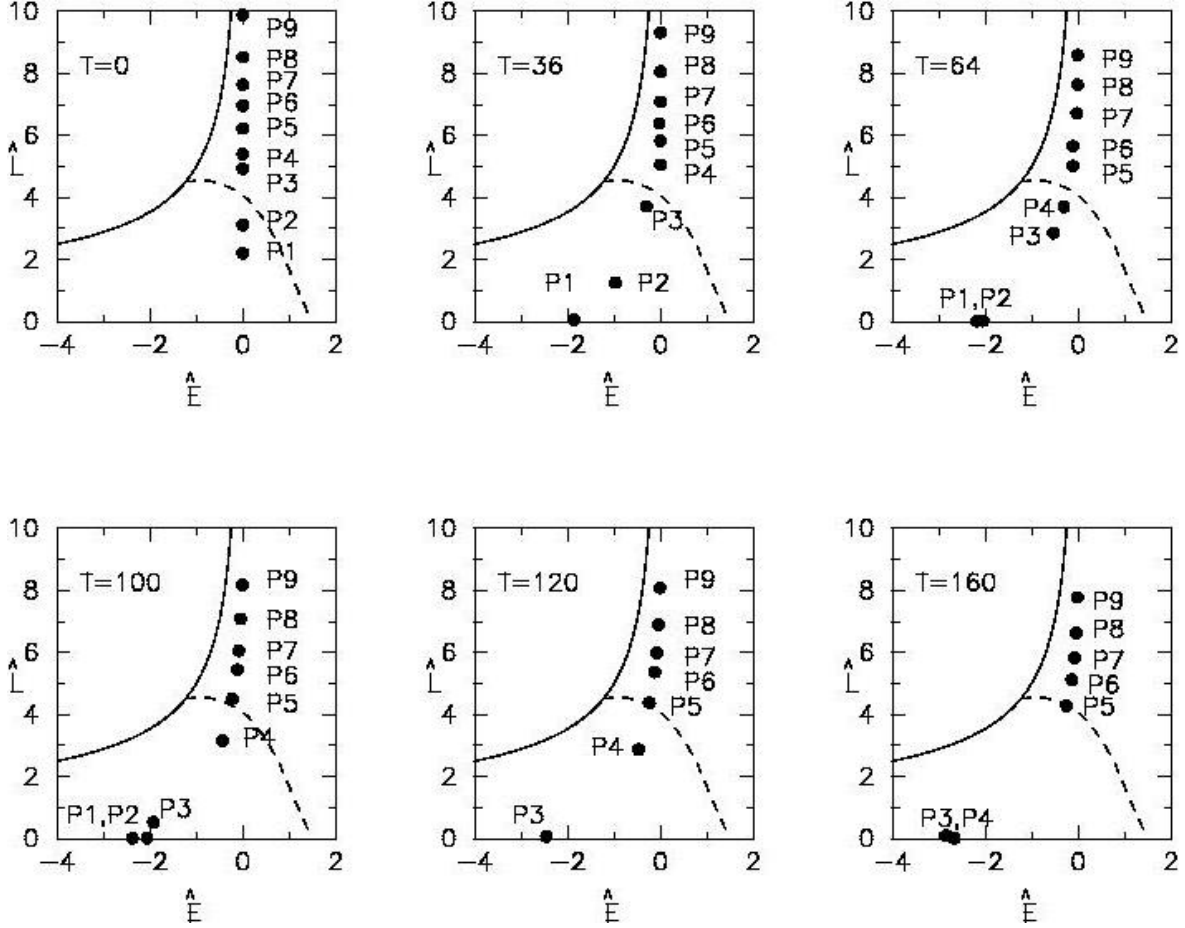


Figure 2. The criterion for merging. The Positions of the models are shown at different times.

Several workers have shown that close collision of two galaxies result in merger if collision velocity is less than the internal velocity dispersion of the galaxies. [25] have shown that the fate of collision of two non rotating galaxies can be determined by two quantities  $\hat{E}$  and  $\hat{L}$  of the initial model where  $\hat{E} = E_{orb}/(0.5 \langle v^2 \rangle)$  and  $\hat{L} = L_{orb}/(R_h \langle v^2 \rangle^{1/2})$  and  $E_{orb}$  and  $L_{orb}$  are the energy and angular momentum per unit mass respectively and  $\langle v^2 \rangle$  is the internal mean square velocity. We show these values plotted for different times during the collision in fig. 2. In this figure the solid curve represents the locus of circular orbits with angular momentum  $\hat{L}$  and energy  $\hat{E}$ . The

dashed curve divides the region of  $(\hat{E}, \hat{L})$  space into two regions viz. merging and non-merging. In the lower portion merging occurs rapidly for bound orbits and within a Hubble time for unbound ones. In the upper region merging occurs more slowly or not at all. The ordinate passing through origin is the locus of parabolic orbit encounters. Initially at  $T = 0$ , all the models lie along this line two of them within the merging region and the rest of them above it. At  $T=36$ , P1, P2 and P3 are within the merging region and P1 has already moved into the rapid merging part. By  $T = 64$ , models P1 – P4 are in the merging region and P1 – P4 are in the merging region and P1 and P2 has already merged into single systems. At  $T = 100$ , P4 also has entered into the merging region and P3 has moved into rapid merging part. By  $T = 160$ , models P3 and P4 have already completed the merging process. Models P6 – P9 do not merge till the end of our computation which is about 60 crossing time. Model P5 which has reached on the boundary of merging region may likely to merge in less than a Hubble time suggesting that the dashed line should be pushed upwards in the case of the specific model considered in this work to accommodate all galaxies that merge in less than a Hubble time.

### 3.3 Features of merger remnant

Initially orbital energy is zero for all the models since collision started off on a relative parabolic orbit. As the collision proceeds, there is considerable loss of orbital energy in models P1 – P4 and consequently the galaxies become bound together. However the merging occurs not during the first close contact time but during the subsequent close contact time only. This can be seen from fig.3, where the separation of the galaxies is plotted as a function of time. The left panel shows the separation of the galaxies in merging simulations and the right panel shows that for the non-merging models. It may be noted that the merging time increases with  $p/R_h$ .

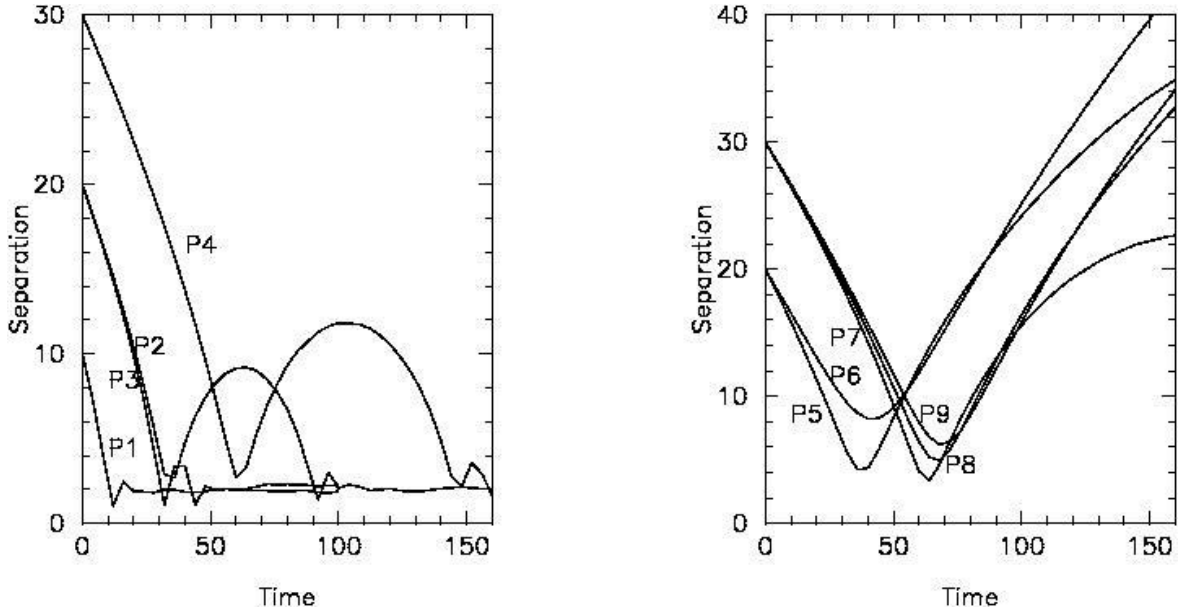


Figure 3. The separation of the galaxies as a function of time.

The amount of energy transferred from the orbit to the internal energy gives an idea about the strength of interaction. The ratio  $\Delta U/|U|$  where  $U$  is the unperturbed initial energy of the galaxy and  $\Delta U$ , its change during an encounter indicate the possible outcome of an encounter. We give these values in table 1.  $\Delta U/|U|$  and  $\Delta M/M$  represent the typical change in the energy and mass of a single galaxy during the encounter.  $\Delta U/|U|$  is maximum for models P1 – P4 indicating that the galaxies undergo considerable disruption before merging.  $\Delta M/M$  for these models is less than 18 per cent (see table 1). Some of the particles leaving one galaxy are captured by the other galaxy and so the effective mass loss  $(\Delta M/M)_E$  is less than 22 per cent. The values of  $(\Delta M/M)_E$  for the merger remnants are given in table 1. For all other models  $\Delta U/|U| < 1$  and  $\Delta M/M$  is less than 8 per cent implying that distant encounters do not produce considerable disruption in the structure of the galaxies.

### 3.4. Density distribution of the remnants

The density distribution in an elliptical galaxy is well fitted with a de Vaucouleur's law

$$\log I(r) = \log I(0) - 3.33[(r/r_e)^{1/4} - 1] \quad (4)$$

Where  $r_e$  is the radius containing half the total light and  $I(0)$  is the brightness at  $r_e$ . This is known as the  $r^{1/4}$  law. We have fitted the above formula to our computed points and the results are shown in fig. 4 for the merger remnants i.e., models P1 – P4. In this figure the open triangles represent the points obtained from our simulations and the best fit is represented by the solid line. The fit is remarkably good over the range in radii where 80 per cent mass of the remnant lies. Departures from  $r^{1/4}$  law occur beyond this radius. This implies that the outer parts show tendency for tidal distension which was observed in several galaxies [26,27].

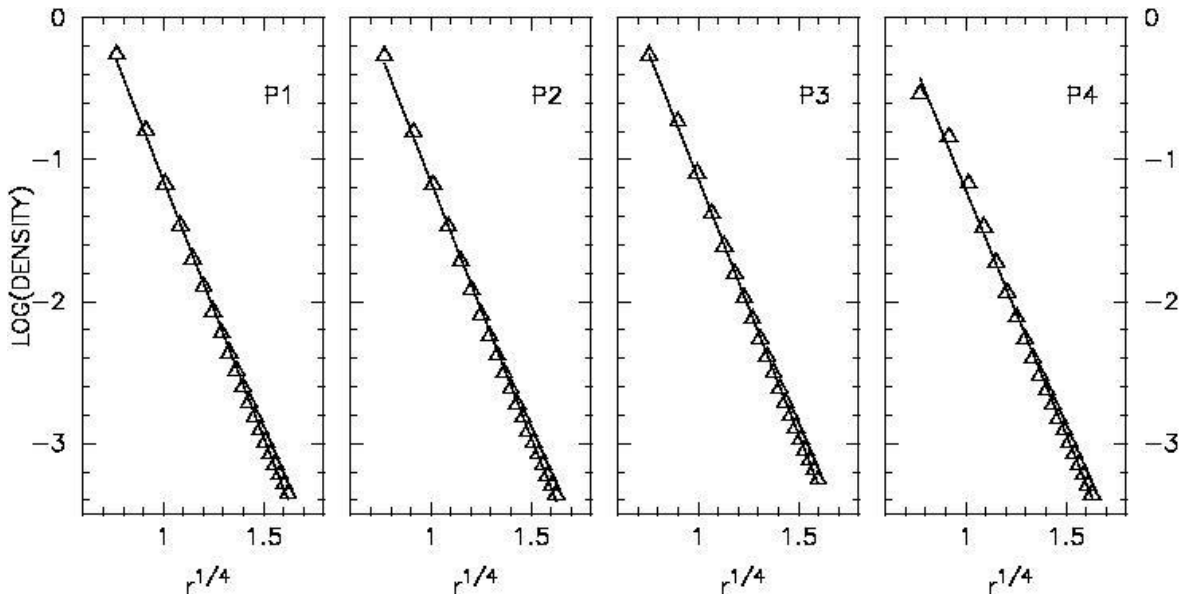


Figure 4. The density distribution in merger remnants. Open triangles are computed points and the solid line represents the best fit.

## 4. Conclusions

Numerical simulations of both merging and non-merging collisions of non-rotating equal mass galaxies have been performed to investigate the effect of changing the impact parameter. The density distribution of the initial model corresponds to that of a polytrope of index  $n = 4$  and the initial relative orbit of the galaxies is parabolic. The hierarchical merging takes place for  $p \leq 3R_h$  and  $V_p \leq 1.1V_e$ . Merging does not take place during the first close contact but during subsequent close contact only. The fate of an collision can fairly well be predicted by computing the relevant values of  $\hat{E}$  and  $\hat{L}$  and plotting them in the  $(\hat{E}, \hat{L})$  plane. The density distribution of the merger remnant can be fitted with the de Vaucouleur's  $r^{1/4}$  law. The fit is remarkably good over a wide range in radius and shows tendency for tidal distension in the outer parts.

## References

1. Alladin, S.M. & Parthasarathy, M., 1978, *Mon. Not. Roy. Astron. Soc.*, 184, 871.
2. Charlton, J.C., Whitmore, B.C. & Gilmore, D.M., 1995, *ASP Conf. Series.*, 70, 49.
3. van Albada, T.S. & van Gorkom, J.H., 1977, *Astron. Astrophys.* 54, 121.
4. White, S.D.M., 1978, *Mon. Not. Roy. Astron. Soc.*, 184, 185.
5. Roos, N. & Norman, C.A. 1979, *Astron. Astrophys.* 70, 75.
6. Aarseth, S.J. & Fall, S.M., 1980, *Astrophys.J.*, 236, 43.
7. Villumsen, J.V., 1982, *Mon. Not. Roy. Astron. Soc.*, 199, 493.
8. Farouki, R.T., Shapiro, S.L. & Duncan, M., 1983, *Astrophys.J.*, 271, 22.
9. Borne, K.D., 1984, *Astrophys.J.*, 287, 503.
10. Navarro, J.F., 1989, *Mon. Not. Roy. Astron. Soc.*, 239, 257.
11. Navarro, J.F., 1990, *Mon. Not. Roy. Astron. Soc.*, 242, 311.
12. Mc Glynn, T.A., 1990, *Astrophys.J.*, 348, 515.
13. Namboodiri, P.M.S. & Kochhar, R.K., 1990, *Mon. Not. Roy. Astron. Soc.*, 243, 276.
14. Barnes, J.E., 1992, *Astrophys.J.*, 393, 484.
15. Hernquist, L., 1992, *Astrophys.J.*, 400, 460.
16. Makino, J. & Hut, P. 1997, *Astrophys.J.*, 481, 83.
17. Funato, Y. & Makino, J., 1999, *Astrophys.J.*, 511, 625.
18. Evstigneeva, E.A., Reshetnikov, V. & Sotnikova, N.Y., 2002, *Astron. Astrophys.* 381, 6.
19. Nopoti, C., Lodrillo, P. & Ciotti, L., 2003, *Mon. Not. Roy. Astron. Soc.*, 342, 501
20. Namboodiri, P.M.S., 2004, *Asian Journal of Physics*, 13, 215.
22. Gonzales-Gracia, A.C. & van Albada, T.S., 2005, *Mon. Not. Roy. Astron. Soc.*, 361, 1030.
23. Makino, J. & Funato, Y., 1993, *Pub. Astron. Soc. Japan*, 45, 279.
24. Dekel, A., Lecar, M. & Shaham, J., 1980, *Astrophys.J.*, 241, 946.



25. Binney, J. & Tremaine, S., 1987, In *Galactic Dynamics*, Princeton University Press, Princeton, New Jersey.
26. Capelato, H.V., De Carvalho, R.R. & Carlberg, R.G., 1995, *Astrophys.J.*, 451, 532.
27. Kormendy, J., 1977, *Astrophys.J.*, 218, 333.